Appl. Phys. B 80, 749–755 (2005)
DOI: 10.1007/s00340-005-1782-9

Applied Physics B
Lasers and Optics

A. COSTELA[1]
I. GARCÍA-MORENO[1]
O. GARCÍA[2,✉]
D. DEL AGUA[2]
R. SASTRE[2]

Structural influence of the inorganic network in the laser performance of dye-doped hybrid materials

[1]Instituto de Química-Física 'Rocasolano', CSIC, Serrano 119, 28006 Madrid, Spain
[2]Instituto de Ciencia y Tecnología de Polímeros, CSIC, Juan de la Cierva 3, 28006 Madrid, Spain

Received: 22 December 2004 /
Revised version: 24 January 2005 /
Published online: 30 March 2005 •

ABSTRACT We report a systematic study of the influence on the laser action of Rhodamine 6G (Rh6G) of the composition and structure of new hybrid matrices based on 2-hydroxyethyl methacrylate (HEMA) as organic monomer and different weight proportions of dimethyldiethoxysilane (DEOS) and tetraethoxysilane (TEOS) as inorganic part. We selected mixtures of di- and tetra-functionalized alkoxides trying to decrease, in a controlled way, the rigidity of the three-dimensional network by making use of the flexibility provided by the linear chains acting as a spacer of the inorganic domains. The organization of the molecular units in these nanomaterials was studied through a structural analysis by solid-state NMR. The different reactivity exhibited by di- and tetra-functionalized silanols generates a non-homogeneous tri-dimensional network. Thus, the laser performance in dye-doped hybrid materials is improved when the inorganic phase is composed of a unique alkoxide.

PACS 42.55.Mv; 42.62.-b; 42.70.-a; 42.70.Hj; 42.70.Jk

1 Introduction

To optimize the laser action of a dye in a solid medium a proper adjustment of the host material structure and composition is required in order to obtain adequate optical, thermal and dynamic–mechanical properties of the matrix. The use of inorganic–organic hybrid systems allows us to combine the excellent thermal properties of inorganic glasses (higher thermal stability, lower thermal expansion and better thermal coefficient of refractive index) [1, 2] with the benefits provided by polymers (good compatibility with organic dyes, optical homogeneity and wide possibilities of modification of structural and chemical composition) [3–6].

Although hybrid matrices have been found where the lasing photostability of dyes such as Rhodamine 6G (Rh6G) and pyrromethene 567 improved significantly with respect to that obtained when these chromophores were incorporated into purely inorganic or organic hosts [6–8], to our knowledge no systematic study of the dependence of the laser action on the structure and composition of the final hybrid material has been carried out. This information would be of great value in the search for strategies to improve the material's photostability.

In a previous work and in order to establish the dependence of the lasing performance on the rigidity and fragility of the final material, we have studied the laser action of Rh6G incorporated into hybrid matrices with monomer (2-hydroxyethyl methacrylate, HEMA) as organic component, and where the proportion and structure of the inorganic compounds were modified in a controlled way [7]. Di-, tri- and tetra-functionalized alkoxides such as dimethyldiethoxysilane (DEOS), methyltriethoxysilane (TRIEOS) and tetraethoxysilane (TEOS), were selected, and the resulting materials were pumped transversely at 534 nm with nanosecond pulses of 5.5 mJ and at a repetition rate of 10 Hz.

Compared with the ditri- and tetra-functionalized alkoxides, the silicon alkoxide with only two reactive positions, which relaxes the rigidity and thus the fragility of the final material, led to the best stability of Rh6G. The decrease of the lasing lifetime as the cross-linked degree of the alkoxide increases could be related to the effect on the lasing properties of the size and morphology of the inorganic domains in the final material. In addition, this behavior could be reflecting the presence of residual water and alcohol generated in the sol–gel process that remain in the matrices due to the soft thermal conditions selected to carry out the polymerization. As a result, TEOS alkoxide leads to the most unstable material, from the structural point of view, since the amounts of water and alcohol generated increase with the number of siloxane groups suitable to be hydrolyzed. When the samples were subjected to a post-polymerization thermal treatment, and thus to a higher degree of dryness, the photostability of the laser operation was significantly improved, confirming the above hypothesis.

The use of DEOS alkoxide leads to linear chains of rapid growth, which results in inorganic domains, less miscible with the organic components, which is detrimental to the optical transparency of the samples and, consequently, to the laser action. For this reason, when the weight proportion of DEOS in the matrix was higher than 10%, the optical quality of the resulting material was not adequate for this application [7]. It is to be expected that the presence of tetra-functionalized

✉ Fax: +34-91-5644853, E-mail: ogarcia@ictp.csic.es

alkoxides should allow an increase of the inorganic content in the host without exceeding the fragility limit of the matrix but improving the flexibility of the cross-linked silanol chains.

Following this idea, and in order to gain more insight into the relationship between the structure of the hybrid matrix and its laser behavior, we proceeded in this work to develop new organic–inorganic hybrid materials incorporating di- (DEOS) and tetra- (TEOS) functionalized alkoxide mixtures which should balance the rigidity of the three-dimensional network through the flexibility provided by the linear chains acting as a spacer in the inorganic domains. The organization of the molecular units in the resulting nanostructured solid materials was studied through a structural analysis by solid-state NMR and its influence on the lasing performance of the dye Rh6G was assessed.

2 Experimental

2.1 *Materials*

Rhodamine 6G (chloride salt, laser grade, Lambda Physik) was used as received with a purity > 99% (checked by spectroscopic and chromatographic methods). 2-hydroxyethyl methacrylate (HEMA) was purchased from Aldrich and was distilled under reduced pressure before use. Dimethyldiethoxysilane (DEOS) and tetraethoxysilane (TEOS) (ABCR, purity of 99%) and hydrochloride acid (35%) (HCl) from Panreac were used as received, without further purification. Minima amounts of distilled water were used to perform the silicon alkoxide hydrolysis. 2,2′-azobis(isobutyronitrile) (AIBN), purchased from Aldrich, was recrystallized in ethanol before use. The molecular structures of dye, alkoxides and monomer molecules selected in this work are shown in Fig. 1.

2.2 *Synthesis*

The synthesis of new organic–inorganic hybrid materials was carried out through the simultaneous and 'in situ' sol–gel process of the inorganic part (TEOS and DEOS), choosing different mixtures of the inorganic precursors [xEOS = yTEOS/(100 − y) DEOS], from 90TEOS/10DEOS to 60TEOS/40DEOS, and the free-radical polymerization of an organic monomer part (HEMA). HEMA was chosen as the pivotal organic component in the formulations since, due to its OH side groups, no addition of solvents was necessary because this monomer acts as a good cosolvent of the selected silicon alkoxides, allowing the maintenance of a viscosity low enough to achieve a good mixing level. In addition, their hydroxyl groups can participate in the polycondensation process of the silanols, improving the organic–inorganic compatibility and allowing an interpenetrated polymer–silica morphology with excellent optical transparency to be obtained.

The sol–gel polymerization of the alkoxide was catalyzed by adding, under continuous stirring, a mixture of water and hydrochloric acid (HCl), maintaining in all cases the following molar ratios: $[HCl]/[x\text{EOS}] = 1.85 \times 10^{-2}$ and $[H_2O]/[x\text{EOS}] = n$, where [xEOS = yTEOS/(100 − y) DEOS] and n was calculated taking into account the different fractions of TEOS/DEOS included in the hybrid as: $n = 2 \times [\text{TEOS}] + 1 \times [\text{DEOS}]$, expressed as a molar fraction. The total content of the silica precursors has been adjusted taking into account the previous results obtained in hybrids with the HEMA/TEOS series incorporating Rh6G [7, 8]. In the present case, this content was varied from 5 wt.% until a maximum of 15 wt.% of xEOS, which allowed us to carry out the synthesis of hybrid monoliths under proper conditions, that is without suffering breaks and maintaining good optical properties.

The theoretical prediction of the total content of silica present in the final hybrid has been calculated assuming that the sol–gel reactions are complete:

$$\text{TEOS}: \text{Si(O–C}_n\text{H}_{2n} + 1)_4 + \text{H}_2\text{O} \rightarrow \text{SiO}_4 + 4\text{C}_n\text{H}_{2n+1} - \text{OH}$$

$$\text{DEOS}: (\text{CH}_3)_2\text{Si(O– C}_n\text{H}_{2n} + 1)_2 + \text{H}_2\text{O} \rightarrow (\text{CH}_3)_2\text{SiO}_2 + 2\text{C}_n\text{H}_{2n+1} - \text{OH}$$

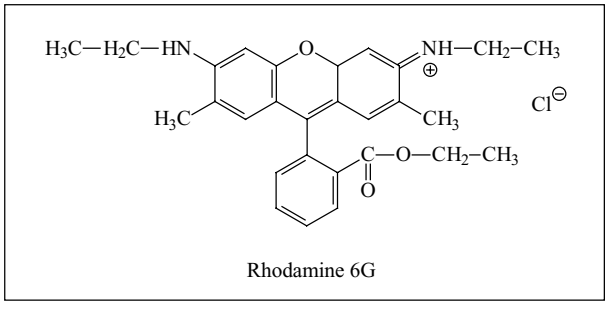

Rhodamine 6G

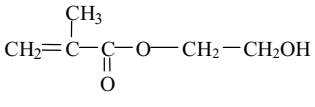

2-hydroxyethyl Methacrylate
(HEMA)

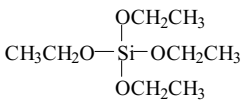

Tetraethoxysilane
(TEOS)

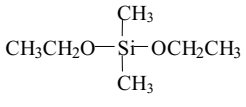

Dimethyldiethoxysilane
(DEOS)

FIGURE 1 Molecular structures of Rh6G dye, organic monomer HEMA and inorganic alkoxides TEOS and DEOS

In these cases, the following equation has been applied [9]:

$$\frac{m_2}{m_1} = \left(\frac{1}{\alpha} - 1\right) \frac{M_{SiO_2}}{M_{x\mathrm{EOS}}},$$

where m_1 and m_2 are the involved masses of the alkoxide mixture and the acrylic monomer, respectively, to be used in the synthesis of the hybrid, α is the silica content of the resulting hybrid (i.e. if a hybrid with a final content of silica of 30 wt.% is going to be synthesized the value of $\alpha = 0.30$) and M_{SiO_2} (≈ 60 g/mol) and $M_{x\mathrm{EOS}}$ are the molecular weight of silica and the average molecular weight of the alkoxide mixture [$M_{x\mathrm{EOS}} = yM_{\mathrm{TEOS}} + (100 - y)M_{\mathrm{DEOS}}$, where $M_{\mathrm{TEOS}} \approx 208$ g/mol for TEOS and $M_{\mathrm{DEOS}} \approx 148$ g/mol for DEOS], respectively.

An adequate amount of Rh6G was dissolved in the corresponding organic monomer mixture to achieve a final concentration of Rh6G of 4×10^{-4} M, and the resulting solutions were placed in an ultrasonic bath to assure the complete dissolution of the dye. The simultaneous organic polymerization was carried out by radical bulk polymerization using a thermal initiator AIBN, in an appropriate concentration (0.5 wt.%) with regard to the total amount of organic monomer in the polymerization mixture. AIBN was the thermal polymerization initiator of choice since it leaves UV-transparent end groups on the so-obtained copolymer.

As an example of the preparation procedure, the detailed steps followed in the preparation of HEMA/*x*EOS–15 wt.% (80TEOS/20DEOS) (the percentage of 15 wt.% is related to the total content of silica present in the resulting hybrid calculated assuming that the sol–gel reactions are complete) were as next described.

First, if a final volume of 6 ml is required, 17 µl of hydrochloric acid solution (35%) and 0.34 ml of water ($[H_2O]/[x\mathrm{EOS}] = (0.8 \times 2) + 0.2 = 1.8$) are added to 0.0085 mol of TEOS (1.77 ml) and 0.0021 mol of DEOS (0.37 ml) under continuous stirring during at least 30 min. On the other hand, 0.028 mol of HEMA (3.4 ml), 0.018 g of AIBN (0.5 wt.%) and the dye (Rh6G, 4×10^{-4} M) are mixed together and filtered using a 0.45-µm pore size filter followed by a 0.2-µm pore size filter (Whatman Lab., polytetrafluoroethylene disposable filters). The final organic solutions were then dropped under stirring on to the TEOS/DEOS solution. The resulting mixture was kept under vigorous stirring for another 30 min. Then, it was poured into cylindrical molds of polypropylene ($\approx$ 14-mm diameter), with the purpose of obtaining a geometric configuration close to that required by the final solid dye laser sample. The molds were then heated in an oven at 45–50°C during $\approx$ 2 months, followed by a slow increasing of temperature, until reaching 80°C, during one week. Finally, the temperature was reduced in steps of 5°C per day until room temperature was reached, and only then were the samples unmolded. Hybrid cylindrical solid monoliths of $\approx$ 3–4 cm^3 were so obtained having both optical transparency and good mechanical properties.

2.3 *Structural analysis by NMR [10–12]*

^{13}C and ^{29}Si NMR experiments were performed in a Bruker Avance™ 400 spectrometer (Bruker Analytik GmbH, Karlsruhe, Germany) equipped with a Bruker UltraShield™ 9.4-T (^{13}C and ^{29}Si resonance frequencies of 100.62 and 79.49 MHz, respectively), 8.9-cm vertical-bore superconducting magnet. In both cases, CP-MAS NMR spectra were acquired at ambient temperature by using a standard Bruker broad-band MAS probe. Representative samples were grounded and packed in 4-mm zirconia rotors, sealed with Kel-F™ caps and spun at 5 kHz. The 90° pulse width was 3.5–4.5 µs and, in all cases, high-power proton decoupling was used. All free-induction decays were subjected to standard Fourier transformation and phasing. The chemical shifts were externally referenced to TMS.

The ^{13}C CP-MAS NMR spectra were acquired with 1-ms CP contact time and 5-s recycle decay. Each spectrum was obtained with 800 averages and 5-Hz line broadening.

The ^{29}Si CP-MAS NMR spectra were obtained with 4-ms CP contact time, 5-s recycle delay, 6000 averages and 75-Hz line broadening. The spectra were deconvoluted by using Gaussian/Lorentzian fits, in terms of Q_i, where $i = 2, 3$ and 4, corresponding to the number of siloxane bridges bonded to the silicon atom of interest. The NMR spectra were evaluated with the software package XWIN-NMR™ provided by Bruker.

2.4 *Methods*

The solid monolith laser samples were cast in a cylindrical shape, forming rods of 10-mm diameter and 10-mm length. A cut was made parallel to the axis of the cylinder to obtain a lateral flat surface of $\approx 6 \times 10\,mm^2$. This surface as well as the ends of the laser rods were prepared for lasing experiments by grinding and polishing until of optical-grade finish. The planar grinding stage was carried out with Texmet 1000 sandpaper (Buehler) using diamond polishing compound of 6 µm as abrasive in mineral oil as lubricant. The final polishing stage was realized with G-Tuch Microcloth (Buehler), using a cloth disk Mastertex (Buehler) with diamond of 1 µm in mineral oil as abrasive type.

The hybrid rods were transversely pumped at 534 nm with 5.5-mJ, 6-ns FWHM pulses from a frequency-doubled Q:switched Nd:KGW laser (Monocrom STR-2+) at a repetition rate of 10 Hz. The exciting pulses were directed towards the lateral flat surface of the sample with a combination of spherical ($f = 50$ cm) and two cylindrical quartz lenses. The first one, with $f = -15$ cm, widened the spherical cross section of the pump beam to illuminate the complete 1-cm length of the dye sample; then, the second lens, with $f = 15$ cm and perpendicularly arranged, focused the pump pulses on to the input surface of the solid sample to form a line of $0.3 \times 10\,mm^2$, so that the pump fluence was 180 mJ/cm^2. The oscillator cavity consisted of a $\approx$ 90% reflectivity flat aluminium mirror and the end face of the solid sample as the output coupler, with a cavity length of 2 cm.

The dye and pump laser pulses were characterized with the following instruments: GenTec ED-100A and ED-200 pyroelectric energy meters, ITL TF1850 fast-rise-time photodiode, Tektronix 2430 digital-storage oscilloscope, SpectraPro-300i monochromator (Acton Research Corporation) and Hamamatsu R928 photomultiplier. The dye and pump laser signals were sampled with boxcars (Stanford Research model

250). All the integrated signals were digitized and processed using a personal computer via a computer board DASH-8 interface [13]. The estimated error of the energy measurements was always less than 10%.

The lasing efficiencies of Rh6G were measured as an average of the first 16 pump pulses at 1 Hz in the different hybrid formulations under study, defined as the ratio between the energy of the dye laser output and the energy of the pump laser incident on the sample surface. The laser stability means the ratio between the intensity of the dye laser output after n pump pulses in the same position of the sample referred to the initial incident intensity.

3 Results and discussion

Solid samples of Rh6G (4×10^{-4} M) incorporated into hybrid matrices of HEMA with mixtures containing different weight proportions of DEOS and TEOS were prepared. In this way, we tested as laser materials a number of hybrid samples with 5, 10 and 15 wt.% proportions of inorganic part added to HEMA. For each of these compositions, the wt.% proportion of TEOS/DEOS in the mixtures ranges from 90/10 to 60/40, which corresponds to increasing the proportions of TEOS and DEOS with respect to HEMA in the final material from 3 to 13.5 and from 0.5 to 6.0, respectively. The following convention is used to represent the new hybrid matrices: HEMA/xEOS-x wt.%, with $x\text{EOS} = (y\text{TEOS}/(100 - y)$ DEOS), x and y representing, respectively, the total weight proportion of inorganic content in the final material and the relative weight proportion of both alkoxides in each composition. Laser emission maxima, oscillation bandwidths and laser efficiency, defined as the ratio between the energy of the dye laser output and the energy of the pump laser incident on the sample surface, are reported in Table 1.

wt.% (HEMA/ xEOS)	wt.% (TEOS/ DEOS)	λ_{max} (nm)	Eff (%)	$I_{100\,000}$ (%)[b]
85/15	90/10	574	12	22
	80/20	582	11	13
	70/30	587	15	18
	60/40	588	10	0
90/10	90/10	571	13	35
	80/20	571	14	39
	70/30	575	11	11
	60/40	576	13	0
95/5	90/10	569	9	43
	80/20	569	10	43
	70/30	570	11	30
	60/40	571	11	21

Dye concentration: 4×10^{-4} M.
[a] λ_{max}: wavelength peak of the laser emission, $\Delta\lambda$: FWHM of the laser emission, Eff: energy-conversion efficiency (as average of the first 16 pump pulses at 1 Hz).
[b] Intensity of the dye laser output after $n = 100\,000$ pump pulses in the same position of the sample referred to the initial intensity I_0, $I_n(\%) = (I_n/I_0) \times 100$.

TABLE 1 Laser parameters[a] for Rh6G dissolved in hybrid matrices of HEMA with TEOS and DEOS alkoxides added in various wt.% proportions, pumped with 5.5 mJ/pulse at 534 nm and 10-Hz repetition rate

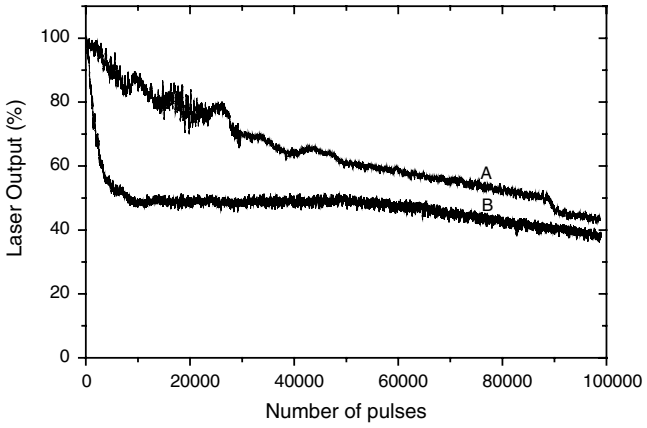

FIGURE 2 Laser output as a function of the number of pump pulses for Rh6G dissolved in HEMA with different wt.% proportions of alkoxide: (A) = 5% and (B) = 10%. In these matrices the inorganic part corresponds to a mixture TEOS/DEOS in a weight proportion of 80/20. Pump energy and repetition rate: 5.5 mJ/pulse and 10 Hz, respectively. Dye concentration: 4×10^{-4} M.

Increasing the inorganic content of the sample as well as the proportion of DEOS in the matrix results in red shifts of the maximum of the laser spectra. These shifts are probably related to changes in the polarity of the medium [14]. Values up to 15% were obtained for the laser efficiency with no clear dependence on the matrix composition.

However, the lasing photostability results are very dependent on the inorganic content of the matrix. In Fig. 2, the dependence of the laser output of Rh6G dye on the number of pump pulses is shown graphically for matrices based on HEMA/xEOS-5 wt.% and HEMA/xEOS-10 wt.% with a proportion 80/20 of TEOS/DEOS. As can be seen in Table 1, for the same TEOS/DEOS weight proportion the lasing photostability increases as the total inorganic proportion in the matrix decreases with respect to the organic content. Likewise, for each HEMA/xEOS ratio the laser photostability decreases as the weight proportion of DEOS in the sample increases with respect to that of the tetra-functionalized alkoxide.

The lasing performances presented in this work improve both our previous results obtained when Rh6G was incorporated into hybrid matrices with DEOS as unique inorganic alkoxide, pumped under otherwise identical experimental conditions [7], and the laser performance reported by other authors for Rh6G incorporated into inorganic and other hybrid hosts [15–21].

Since the new hybrid materials developed in this work are synthesized starting from two different inorganic precursors, linear and/or cross-linked networks could be generated. The solid-state ^{29}Si NMR analysis would provide evidence of the formation of these hybrid networks and also yield information concerning the chemical structure and degree of condensation of the materials. As an example, a ^{29}Si NMR spectrum of the hybrid material HEMA/xEOS-15 wt.% (70TEOS/30DEOS) is shown in Fig. 3. Four peaks appear at −15, −92, −101 and −109 ppm. The three signals centered at −92, −101 and −109 ppm correspond to Q_2, Q_3 and Q_4 species, respectively. The assignment of these peaks is based on previous studies of silica gels [22] and agrees with those obtained in our previous

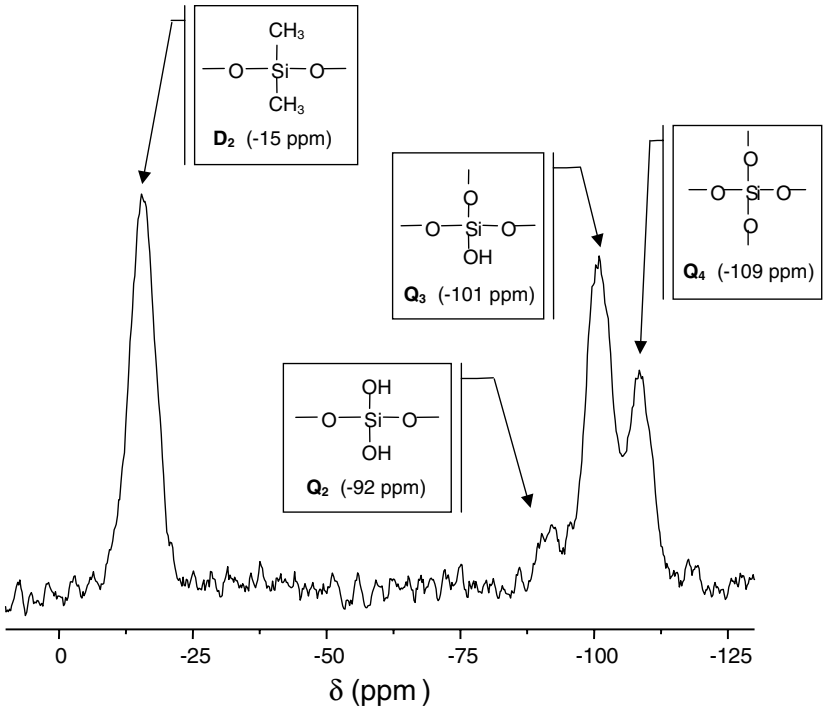

FIGURE 3 ^{29}Si CP-MAS high-power proton decoupling NMR spectrum corresponding to a sample of the hybrid HEMA/*x*EOS-15 wt.% (70TEOS/30DEOS). The spectrum was obtained with 6000 averages, a 5-s recycle delay and a line broadening of 75 Hz. The resonances at −92, −101 and −109 ppm correspond to silicons from TEOS with two, three and four siloxane bonds to the silicon of interest, and the resonance at −15 ppm corresponds to silicons from DEOS with two siloxane bonds to the silica network

structural analysis of hybrid materials based on 5–30 wt.% HEMA/TEOS [8].

The peak at −92 ppm corresponds to the Q_2 species and is assigned to the silicon atom bonded to two –OH groups and two other siloxane groups, represented by $SiO_2(OH)_2$. The peak Q_3 at −101 ppm is related to the presence of a silanol group bonded to the inorganic structure of type SiO_3OH and, finally, the Q_4 peak at −109 ppm is associated with silicon bonded to four siloxane groups, such as SiO_4 [23].

In addition, the new peak centered around −15 ppm is assigned to a new D_2 species, induced in this new hybrid material as a consequence of the presence of DEOS, and attributed to the silicon atom bonded to two siloxane groups and two methyl groups, represented by $SiO_2(CH_3)_2$ and corresponding to the polycondensation of DEOS to form linear microdomains of silica [24]. The D_2 peak shifts from −14 ppm (90TEOS/10DEOS) to −16 ppm (60TEOS/40DEOS) due to the silicon in the siloxane segments of growing length. On the basis of the quantitative relationship of these signals, which are comparable under the same experimental conditions, it is observed that as the content of DEOS in the hybrid material increases with respect to TEOS, the relative proportion of D_2 species increases (from 15.7% in 90TEOS/10DEOS, 44.1% in 70TEOS/30DEOS to 48.3% in 60TEOS/40DEOS hybrids) as both the Q_2 and, more significantly, the Q_3 species decrease. This result would suggest that DEOS is actually acting as a spacer agent in the inorganic three-dimensional network. In this way, the increase of DEOS proportion in the hybrid material results in an increase of the relative final proportion of the totally polycondensated silicon (Q_4) species (Fig. 4), since the silanol groups from DEOS can only react with themselves or with silanols present in Q_2 and Q_3 species, to become Q_3 and Q_4, respectively.

No more peaks appear in the CP-MAS ^{29}Si NMR spectra due to the presence of a silicon monocondensated group (D_1 or Q_1 species) or silicon bonded to an organic group in the different chemical environments studied. However, the chemical bond formation in the polycondensation between silica and hydroxyl groups of the organic mononer (HEMA) could be confirmed through CP-MAS ^{13}C NMR, which probes that a true bond exists between the inorganic and organic domains explaining the homogeneous optical properties of the so-obtained hybrid materials [8].

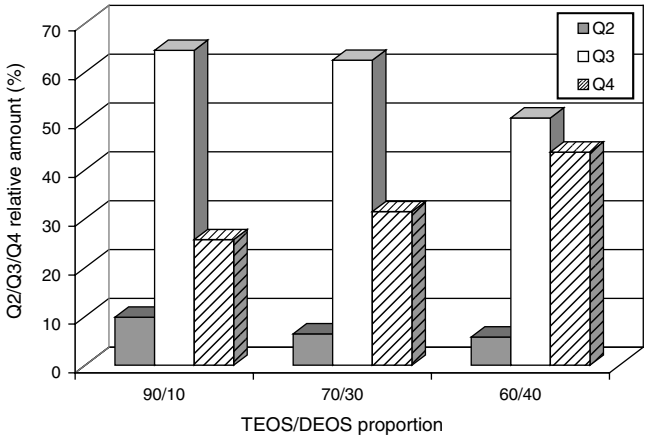

FIGURE 4 Relative relationship of the signals, comparable under the same experimental conditions, for species Q_2, Q_3 and Q_4 in the hybrid samples HEMA/*x*EOS-15 wt.% with different proportions of TEOS/DEOS

Keeping in mind the theoretical prediction of the assignment of ^{13}C, if there was polycondensation between the organic and inorganic phases a new peak at 64.5 ppm should be observed [25]. As shown in Fig. 5, a very small but defined peak is detected at 64 ppm, shielded by two other big peaks hindering its quantification. The intensity of this signal decreases as the DEOS proportion in the hybrid matrix increases although, within the experimental resolution, it is

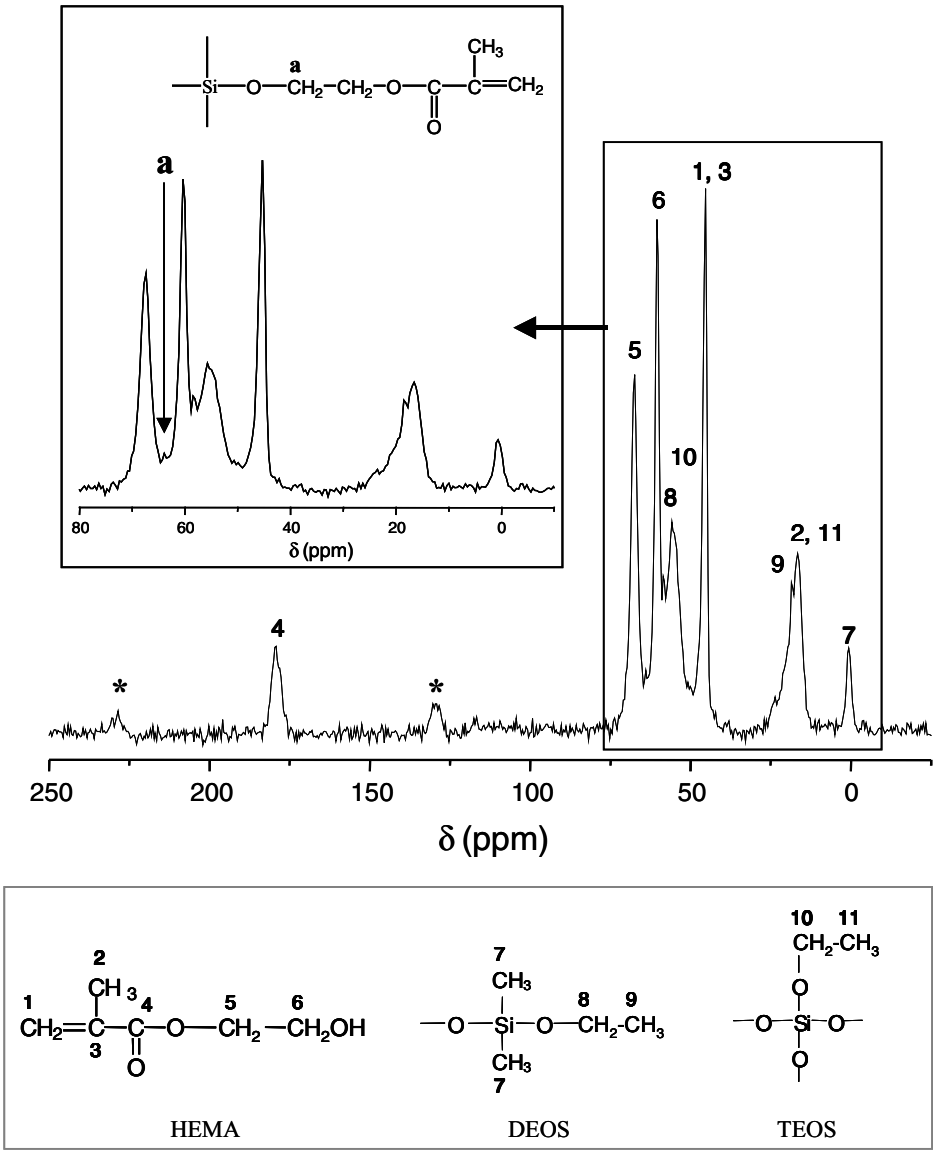

FIGURE 5 ^{13}C CP-MAS high-power proton decoupling NMR spectrum corresponding to a sample of hybrid HEMA/*x*EOS-15 wt.% (70TEOS/30DEOS). The spectrum was obtained with 800 averages, a 5-s recycle delay and a line broadening of 5 Hz. The *inset* shows the vertical expansion of the spectrum between 0 and 80 ppm. The resonance observed at 64 ppm might be associated with the presence of a chemical moiety produced by the chemical bonding between the organic and inorganic phases. The spinning side bands corresponding to the peak associated with the carbonyl group are indicated with *. Each peak represented in the CP-MAS ^{13}C NMR spectrum can be assigned to the different carbon groups present in the hybrid system according with the theoretical prediction of the assignment of ^{13}C in each precursor (organic and inorganic)

not possible to assure that it disappears completely. No more peaks that assure the interactions between HEMA and DEOS are detected.

Since the structural analysis of these hybrid materials reveals that DEOS silanols neither increase the compatibility with the organic phase of the material nor act significantly as spacer agents in the three-dimensional inorganic network, we proceeded to synthesize and characterize several samples of Rh6G dissolved in hybrid matrices of HEMA with TEOS as unique alkoxide added in wt.% proportions ranging from 1% to 10%. The evolution of lasing efficiency and stability with the proportion of TEOS is reported in Table 2. Following the same behavior as that observed for the hybrid materials containing TEOS/DEOS, values up to 19% were obtained for the laser efficiency with no clear dependence on the matrix composition. However, the lasing photostability results are very dependent on the inorganic content of the matrix, with the lasing lifetime decreasing with the proportion of TEOS. The highest laser lifetime was reached for the composition with only 1 wt.% of the alkoxide.

The photostabilities reached for Rh6G dissolved in hybrid matrices of HEMA with low weight proportions of TEOS are higher than those obtained with mixtures of TEOS/DEOS. This behavior could be related to the high reactivity of DEOS that leads preferentially to linear chains of rapid growth rather than to the spreading out of tetra-functionalized domains

Material TEOS wt.%	λ_{max} (nm)	$\Delta\lambda$ (nm)	Eff (%)	$I_{100\,000}$ (%)[b]
1%	569	6	16	110
3%	569	5	13	65
5%	581	7	19	50
10%	594	7	18	0

Dye concentration: 4×10^{-4} M. Nd:YAG pump energy: 5.5 mJ/pulse, repetition rate: 10 Hz.
[a]λ_{max}: wavelength peak of the laser emission, $\Delta\lambda$: FWHM of the laser emission, Eff: energy-conversion efficiency (as average of the first 16 pump pulses at 1 Hz).
[b]Intensity of the dye laser output after $n = 100\,000$ pump pulses in the same position of the sample referred to the initial intensity I_0, $I_n(\%) = (I_n/I_0) \times 100$.

TABLE 2 Laser parameters[a] for Rh6G incorporated into hybrid matrices of HEMA with different weight proportions of TEOS

and to the chemical bond formation by polycondensation between silica and hydroxyl groups of HEMA.

The systematic study carried out in this work reveals that, in solid-state dye lasers based on hybrid matrices, the structural homogeneity of the inorganic phase is a factor more important than the rigidity of the corresponding three-dimensional network to enhance the laser action. Consequently, the dye-doped hybrid materials should be based on a monomer or mixture of monomers as organic phase but on a unique alkoxide as inorganic part since otherwise the different reactivities exhibited by the di- and tetra-functionalized alkoxides generates a more heterogeneous inorganic network, as confirmed by the structural analysis by solid-state NMR, which impairs the laser action.

ACKNOWLEDGEMENTS This work was supported by Project No. 7N/01000/02 of Comunidad Autónoma de Madrid (CAM). D. del Agua thanks CAM for his predoctoral grant and O. García wishes to thank the Ministerio de Ciencia y Tecnología (MICYT) for awarding him a Ramón y Cajal postdoctoral contract.

REFERENCES

1 D.N. Nikogosian, *Properties of Optical and Laser-Related Materials: A Handbook* (Wiley, New York, 1997), pp. 388–391
2 N.P. Barnes, Transition metal solid-state lasers. In *Tunable Laser Handbook*, ed. by F.J. Duarte (Academic, San Diego, 1995), pp. 219–291
3 F.J. Duarte, Appl. Opt. **33**, 3857 (1994)
4 R. Sastre, A. Costela, Adv. Mater. **7**, 198 (1995)
5 M.D. Rahn, T.A. King, J. Mod. Opt. **45**, 1259 (1998)
6 A. Costela, I. García-Moreno, R. Sastre, in *Materials for Solid-State Dye Lasers*, ed. by H.S. Nalwa. Handbook of Advanced Electronic and Photonic Materials and Devices, vol. 7 (Academic, San Diego, 2001), pp. 161–208
7 A. Costela, I. García-Moreno, C. Gómez, O. García, R. Sastre, Appl. Phys. B **78**, 629 (2004)
8 A. Costela, I. García-Moreno, C. Gómez, O. García, L. Garrido, R. Sastre, Chem. Phys. Lett. **387**, 496 (2004)
9 P. Hajjl, L. David, J.F. Gerard, J.P. Pascault, G. Vigier, J. Polym. Sci. Part B: Polym. Phys. **37**, 3172 (1999)
10 T. Tanaka, in *Experimental Methods in Polymer Science*, vol. 4, ed. by T. Tanaka (Academic, San Diego, 1998), pp. 310–330
11 L. Garrido, Rev. Plást. Mod. **83**, 485 (2002)
12 P.A. Mirau, Rapra Rev. Rep. **11**(8), 128 (2001)
13 M. Rodríguez, A. Costela, I. García-Moreno, F. Florido, J.M. Figuera, R. Sastre, Meas. Sci. Technol. **6**, 971 (1995)
14 G. Quian, Z. Yang, C. Yang, M. Wang, J. Appl. Phys. **88**(5), 2503 (2000)
15 J.C. McKiernan, S.A. Yamanaka, B. Dunn, J.I. Zink, J. Phys. Chem. **94**, 5652 (1990)
16 E.T. Knobbe, B. Dunn, P.D. Fuqua, F. Nishida, Appl. Opt. **29**, 2729 (1990)
17 J.C. Altman, R.E. Stone, B. Dunn, F. Nishida, IEEE Photon. Technol. Lett. **3**, 189 (1991)
18 D. Larrue, J. Zarzycky, M. Canva, P. Georges, F. Bentivegna, A. Brun, Opt. Commun. **110**, 125 (1994)
19 M.D. Rahn, T.A King, Appl. Opt. **34**, 8260 (1995)
20 L. Hu, Z. Jiang, Opt. Commun. **148**, 275 (1998)
21 S. Schultheiss, E. Yariv, R. Reisfeld, H.D. Breuer, Photochem. Photobiol. Sci. **1**, 320 (2002)
22 C.A. Fyfe, Y. Zhang, P. Araca, J. Am. Chem. Soc. **114**, 3252 (1992)
23 M.G. Fonseca, A.S. Oliveira, C. Aiiroldi, J. Colloid Interface Sci. **240**, 533 (2001)
24 G.P. Wang, T.C. Chang, Y.S. Hong, Y.S. Chiu, Polymer **43**, 2191 (2002)
25 A. Herrera, R. Martínez, *Tablas para la Determinación Estructural por Métodos Espectroscópicos* (Springer, Barcelona, 1998)